

A 45 AU RADIUS SOURCE AROUND L1551–IRS 5: A POSSIBLE ACCRETION DISK

J. Keene¹ and C. R. Masson^{1,2}

¹*California Institute of Technology, 320-47, Pasadena, CA, 91125, USA*

²*Center for Astrophysics, 60 Garden Street, Cambridge, MA, 02138, USA*

Abstract. Our interferometric and single-dish observations of the continuum emission from L1551–IRS 5 show that, at millimeter wavelengths, there are two distinct components to the source, an envelope with a radius ≥ 2000 AU, and a compact core with a radius ≤ 64 AU. The compact core has a large optical depth, indicating a high column density ($\sim 1000 \text{ g cm}^{-2}$). By modeling the temperature in the region of the compact core, we show that its size must lie in the range 45 ± 20 AU. The compact core is most plausibly identified with an accretion, or preplanetary, disk around the star, although the present observations do not have sufficient angular resolution to rule out other structures.

1. Introduction

The immediate circumstellar environment of protostars is the most important and least understood influence on the process of star formation. During gravitational collapse of material with nonzero angular momentum, it is likely that a disk will form around the protostar (e.g., Cameron 1985; Safronov and Ruzmaikina 1985; Lin and Papaloizou 1985; Hayashi, Nakazawa, and Nakagawa 1985). The rate of accretion on to the forming star is then controlled by the viscosity in the disk which permits angular momentum to be transferred outward and allows some of the disk material to fall on to the star. At some stage during the process, a strong wind develops, giving rise to a bipolar outflow of material, probably terminating accretion on to the star. Since, for energetic reasons, these winds must originate very close to the stellar surface, the accretion disk almost certainly plays an important role in producing the strong collimation often observed. In the final stages of evolution, planetary systems are believed to be formed from condensations in the remnant disk material.

Despite the vital role expected for such disks in all aspects of the formation and growth of low-mass stars, there is very little direct evidence about their nature. The most direct observation of a circumstellar disk is provided by the observations of Smith and Terrile (1985) of a thin, ~ 400 AU radius disk around the star β Pic, presumably the remnant of a more massive protostellar accretion disk. Estimates of outer radii of accretion disks give values of $\sim 10 - 100$ AU, (e.g., Adams, Lada, and Shu 1987), corresponding to angular radii of $0''.07 - 0''.7$ in the nearest star-forming regions, a scale which is difficult to resolve with most astronomical instruments. Indirect evidence for their nature comes from the existence of the solar system. From the elemental abundances found in the planets, it can be estimated that the disk of the presolar nebula must

have extended at least to a radius of 40 AU and must have contained at least $0.02 M_{\odot}$, just to account for the material in the planets (e.g., Safronov and Ruzmaikina 1985 and references therein).

One of the best known examples of a young star which is still deeply embedded in its parent cloud is the object IRS 5 in the L1551 dark cloud. This object has one of the most spectacular bipolar molecular outflows observed (Snell, Loren, and Plambeck 1980). The outflow lobes extend to a distance of $\gtrsim 10'$ ($\gtrsim 0.5$ pc at the assumed distance of 160 pc; Snell 1981) from the central star and are well collimated on this scale. Near-infrared observations (Campbell *et al.* 1988) show that the outflow is well collimated even at a distance of $1''$ (160 AU) from the central star. VLA cm continuum observations (Bieging, Cohen, and Schwartz 1984; Bieging and Cohen 1985; Rodríguez *et al.* 1986) show that there is a well-collimated jet of ionized material, with a diameter of $0''.5$ extending right to the center of the source.

Most of the material in the immediate environment of IRS 5 is molecular and is not detected by continuum observations at the VLA, while high obscuration impedes optical and infrared studies. The most sensitive tool for investigation of such material is continuum emission from dust grains, which is usually optically thin in the millimeter wavelength range and therefore provides the best tracer of the column density of material. Spectral line observations can provide velocity information, but the available resolution is limited by the sensitivity available in the small line widths.

2. Observational Results

We have mapped L1551 in the continuum at 2.73 mm at high spatial resolution with the Owens Valley Radio Observatory (OVRO) millimeter-wave interferometer. We have measured the 1 mm continuum flux density with the 5 m Hale telescope at Palomar Observatory and mapped the 1.25 mm continuum with the 10.4 m Caltech Submillimeter Observatory (CSO).

The observed flux densities are presented in Table 1. We have estimated the calibration uncertainties to be 20% and have added that in quadrature to the statistical noise.

TABLE 1

L1551 OBSERVATIONS

Wavelength (mm)	Peak Flux Density (Jy beam ⁻¹)	Beam Size ($''$)
1.0	5.7 ± 1.3	55
1.25	2.37 ± 0.48	27
2.73	0.13 ± 0.03	2.7×2.6

2.1. CSO Map at 1.25 millimeters

Figure 1 shows the 1.25 mm map of L1551 made at the CSO in 1988 September with a $27''$ beam (FWHM). Although no structural details can be discerned in Figure 1, it shows that L1551 is spatially resolved; Gaussian deconvolution gives a diameter of $24''$ (FWHM). Our measurements are in good agreement with similar recent data by Walker, Adams, and Lada (1990) and indicate that a substantial amount of the dust emission arises in an envelope with an radius of ~ 2000 AU.

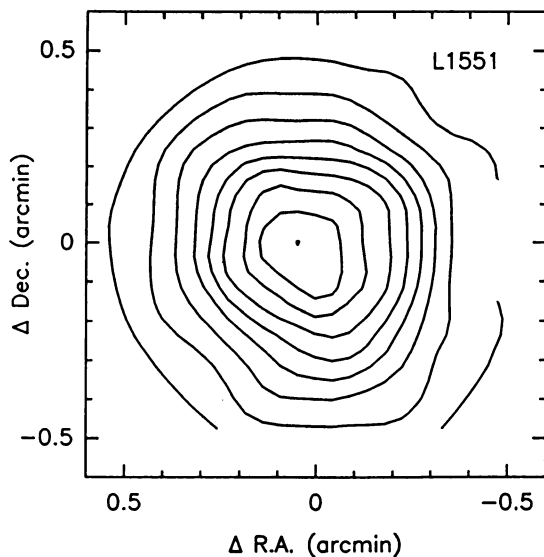


Fig. 1. 1.25 mm map of L1551–IRS 5 taken with $27''$ resolution at the CSO. The peak flux in this map is 2.37 Jy per beam and the rms noise is ~ 0.06 Jy. The Gaussian deconvolved source size is $24''$ (FWHM). The contour levels are spaced by 10%, starting at 20% of the peak flux; the 10% contour lies outside the mapped area. The lowest contour is 8.5σ .

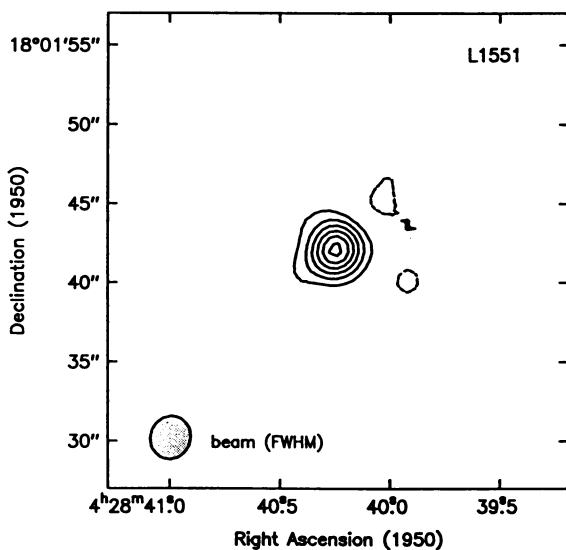


Fig. 2. 2.73 mm map of L1551–IRS 5 taken with $2''.7 \times 2''.6$ resolution at OVRO. The peak flux density in this map is 130 mJy per beam and the integrated flux is 150 mJy; the contours are 20 mJy. The rms noise in the map is 5 mJy per beam.

2.2. OVRO Interferometer Map at 2.73 millimeters

Figure 2 shows the map of the 2.73 mm continuum emission of the L1551–IRS 5 area made from only the best 3 days of data. The beam size is $2''.7 \times 2''.6$. Because the minimum projected baseline in this dataset was 35 m, structures with scale sizes $\gtrsim 10''$ are resolved out. Thus the interferometer map shows only a strong pointlike source despite the evidence presented above from the single-dish measurements that there also exists a large envelope. The center of the 2.73 mm source is at $04^{\text{h}} 28^{\text{m}} 40^{\text{s}}.25, +18^{\circ} 01' 42''.2$ (1950) and is coincident with the position of the radio continuum sources mapped by Rodríguez *et al.* (1986).

The presence of the extended envelope, seen at 1.25 mm with the CSO, complicates attempts at deconvolution to determine the size of the compact core seen by the interferometer. A limit on the source size can be found by considering the measured visibility amplitudes plotted in Figure 3. In this figure, the observed visibility amplitudes from the entire 1986–87 season were vector averaged over 1 hr periods and then binned at regular u - v intervals (and thus azimuthally averaged). The error bars represent only the scatter among the vector-averaged points. At the shortest baselines the visibility amplitudes increase due to the extended envelope which is heavily resolved by the interferometer; at larger baselines the visibility amplitudes are approximately constant, although there is a slight falloff with increasing baselines.

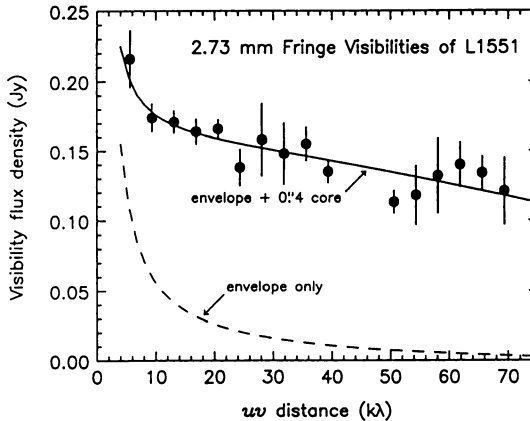


Fig. 3. The observed 2.73 mm visibilities. The dashed line shows the visibilities resulting from an envelope with 0.29 Jy total flux and with a volume emissivity $\propto r^{-2}$. The solid line shows the visibilities resulting from a similar envelope with a flux of 0.14 Jy plus a compact Gaussian source with a flux of 0.15 Jy (for a total flux of 0.29 Jy) and a half-power radius of $0''.4$. It is obvious that the two-component model (solid line) fits the data much better than a simple power-law source.

For comparison we have computed the visibility spectrum of a $\rho \propto r^{-3/2}$ power-law envelope as predicted by Terebey, Shu, and Cassen (1984) for the collapse of a slowly rotating, spherical, isothermal cloud. The temperature profile was assumed to have a power-law form, $T \propto r^{-1/2}$. In the Rayleigh-Jeans limit, the source volume emissivity, therefore, is proportional to r^{-2} . The total flux density (0.29 Jy within a $60''$ beam) was interpolated between our 1.0 mm measurement and that of Walker, Adams, and Lada (1990) at 2.9 mm (Table 2). The lower curve in Figure 3 (*dashed line*) shows the visibility for this power-law envelope; it falls far short of the data at large baselines. Varying the power-law index changes the shape of the curve slightly, but for no power-law index can the predicted flux densities be made to match both the visibility amplitudes and

the large beam flux. The large visibility amplitudes seen at large baselines therefore demonstrate that the compact core detected by the interferometer is a discrete structure and cannot be simply the dense, central part of a power-law envelope.

A good fit to the data in Figure 3 can be obtained, however, by using a two-component model, with a power-law envelope to account for the rise in flux density at short baselines and a compact core to account for the large flux in the long-baseline data. The solid curve plotted through the data points consists of a power-law envelope plus a compact circular Gaussian source. This two component model fits the observations very well. The small decrease in the visibility amplitudes at large baselines gives an estimate of the size of the compact core; the plotted curve is derived from a compact source with a half-power radius of $0''.4$ and a flux density of 0.15 Jy. Again, the total flux in a $60''$ beam was taken to be 0.29 Jy (Table 2). To fit the data only the size and total flux of the compact core were allowed to vary. This size for the compact core derived from Figure 3 is much more realistic than a simple Gaussian fit to the interferometer map because the effect of the envelope is taken into account, but it is still subject to observational errors which are likely to reduce the measured amplitudes on the longest spacings. Therefore we regard $0''.4$ (64 AU) as an *upper limit* to the radius of the compact core.

Using the upper limit for the size of the compact core, we can calculate the lowest brightness temperature required to produce the observed flux densities. For a circular Gaussian source with a radius of $0''.4$ and an integrated flux density at 2.73 mm of 150 mJy, the peak Rayleigh-Jeans brightness temperature is 24 K. If the source size is the same at 1.36 mm, the required brightness temperature is 28 K to produce the observed flux density of 0.7 Jy (Woody *et al.* 1989). If the compact core is actually smaller than $0''.4$ in radius, then the brightness temperature must be correspondingly higher. In §4.2 below we use an upper limit to the source temperature to derive a lower limit of $0''.16$ to the source radius.

3. Continuum Energy Distribution of L1551

The continuum energy distribution of L1551–IRS 5 (Fig. 4) shows a large far-infrared luminosity characteristic of thermal emission from dust grains and a relatively flat centimeter wavelength spectrum characteristic of optically thin free-free emission from ionized gas. Integration under a smooth curve fitted through only the points measured with large beam sizes ($> 25''$) gives a total luminosity for L1551–IRS 5 of $33 \pm 3 L_{\odot}$ for the assumed distance of 160 pc.

In Table 2 we separate out the contributions of the compact core and the envelope to the total flux in the mm wavelength region. To do this we have used the observed flux densities to calculate the spectral indices of the total flux and of the compact core, then interpolated or extrapolated to the unobserved frequencies. For the compact core we have used only the 1.36 and 2.73 mm measurements for the interpolation since they were made with the smallest beam sizes. Subtraction of the compact core from the total flux gives us the envelope flux.

The compact core has an observed spectral index of 2.4 ± 0.5 over the range from 1.36 to 2.73 mm, and the Planck correction should be negligible at the temperatures expected 64 AU from the central star. This spectral index is close to the value of 2 expected for optically thick thermal emission. The inferred spectral index of the envelope between 1.0 and 2.9 mm is 3.3 ± 0.7 . The dust in the envelope has a relatively low temperature and a Planck correction must be made to calculate the emissivity law of the dust. If the mean temperature of this material is taken to be 25 K, the emissivity law has a slope of 1.5 ± 0.7 , in adequate agreement with the theoretically expected value of 2.0 (see e.g., Draine and Lee 1984).

TABLE 2

ADOPTED FLUX DENSITIES FOR L1551

Wavelength (mm)	Total ^a (Jy)	Core ^b (Jy)	Envelope (Jy)
1.0	5.7 ^c	1.5	4.2
1.36	2.3	0.7 ^d	1.6
2.73	0.29	0.13 ^e	0.16
2.90	0.24 ^f	0.11	0.13

^a Assumes, unless measurement is indicated, that $F_\nu \propto \nu^{3.0}$.

^b Assumes, unless measurement is indicated, that $F_\nu \propto \nu^{2.4}$.

^c This work, 55'' beam.

^d Woody *et al.* 1989; 3'' beam.

^e This work, 2.''7 × 2.''6 beam.

^f Walker, Adams, and Lada 1990; 60'' beam.

4. The Structure of L1551–IRS 5

The most detailed modeling of the emission from sources such as L1551–IRS 5 has been performed by Adams and Shu (1986), who have successfully reproduced the observed energy distribution with a model of an infalling envelope resulting from the symmetrical collapse of a rotating, spherical, isothermal cloud (Terebey, Shu, and Cassen 1984). In these models, the infalling envelope has a power-law density distribution outside the radius where rotation becomes significant. Inside this radius, the infalling material forms an accretion disk as it spirals in toward the central star. The luminosity arises, in general, from three different sources, nuclear burning in the central star, dissipation of gravitational potential energy in the accretion disk, and the accretion shock, where the orbiting material at the inner edge of the disk meets the surface of the star. In their model, the emission from the central star and accretion disk was used only to heat the envelope, and the appearance of the disk itself was not considered in detail. Since the interferometer data presented here show evidence for a compact core in addition to the envelope, we have identified the compact core with the disk and have attempted to model the appearance of this disk as well as the extended envelope. In this section, we analyze the available spectral and mapping data to identify what constraints they place on models of the source, and we present a simplified model which has the essential characteristics required to account for the observations.

We assume that dust emission is represented by an opacity law of the form described by Keene, Hildebrand, and Whitcomb (1982) and Hildebrand (1983). The low-frequency opacity ($\lambda > 100 \mu\text{m}$) is taken to be $\tau = 1.3 \times 10^{-26} N_H \lambda_{\text{mm}}^{-2}$ ($\text{cm}^2 \text{atom}^{-1} \text{mm}^2$), which gives rise to an energy distribution of the form $F_\nu \propto \nu^4$ in the Rayleigh-Jeans limit and which is in good agreement with the characteristics of the extended envelope discussed in the previous section. Although we find a shallower slope for the emission from the compact core in L1551, we show below that this slope can plausibly be accounted for by the effects of high optical depth. In general, the sources which are detectable by interferometers at low frequencies are those in which brightness temperatures and optical depths are high; opacity effects are therefore important and the dust emissivity law cannot simply be inferred from the slopes of the observed spectra.

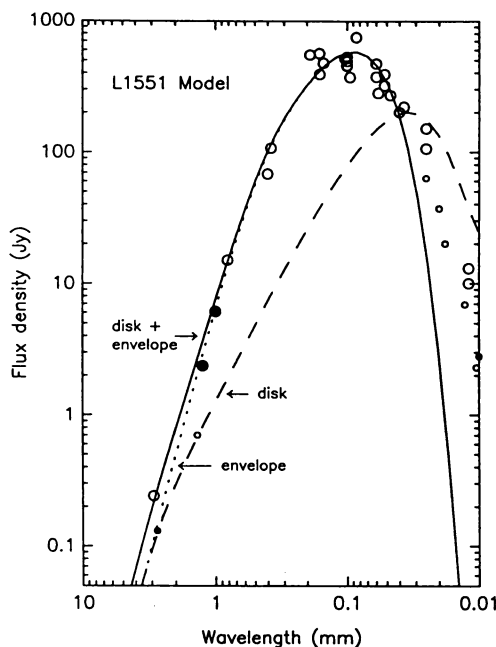


Fig. 4. Curves representing simple models for the compact core and envelope and the combined energy distribution plotted with the observations. The dashed curve shows the flux from the model disk; the dotted curve shows the flux from the model envelope; the solid curve shows the flux from the disk/envelope combination. Filled symbols indicate flux densities obtained in this work; large symbols indicate flux densities obtained with beam sizes $> 25''$; small symbols indicate flux densities obtained with beam sizes $< 25''$.

4.1. Envelope

In Figure 4 we plot the observed fluxes of L1551, where we take the large beam measurements to be observations of the core/envelope combination and the interferometric measurements at mm wavelengths to be measurements only of the core, along with curves representing simple models for the core and envelope separately. For simplicity, the plotted model for the envelope consists of a homogeneous sphere of material with a total mass of $1.12 M_{\odot}$, a radius of $1''.5$ (240 AU), and a temperature of 57 K. The total mass is constrained by the long wavelength data points where the envelope emission is optically thin and the radius and temperature were taken to be those where the Planck-averaged optical depth of the envelope becomes small (i.e., to fit the observed emission peak). This model does not account for the extended nature of the envelope, which makes single-dish millimeter wavelength maps appear extended (e.g., Fig. 1), but it does give a rough estimate of the temperature and mass of envelope material. However, the total mass of the envelope is probably larger by a factor of 2–3 than assumed in the model because the bulk of the envelope material is far from the central star and has a lower temperature than that derived from the emission peak. The size and mass of the envelope are poorly defined, since it blends into the surrounding cloud, but the total mass is probably 2–3 M_{\odot} within a radius of ~ 2000 AU.

4.2. Compact Core

The compact core has been measured only between 1.36 and 3.4 mm, and in this wavelength

region has a spectral index of ~ 2.4 . The simplest explanation for this index is that the compact component is so condensed that the material is optically thick at a wavelength of 1.36 mm and has $\tau \sim 1$ at 2.73 mm. An argument in favor of this explanation is the large brightness temperature calculated for the compact core. At a radius of $0''.4$ (64 AU) from the central star, the characteristic temperature, $(L_*/4\pi\sigma r^2)^{1/4}$, should be ~ 120 K. Based on our upper limit of $0''.4$ for the radius of the compact core, we calculate a Rayleigh-Jeans brightness temperature of > 24 K at 2.73 mm, indicating that the optical depth through the compact core must be *at least* 0.2; it could be significantly greater if the compact core radius is much smaller than $0''.4$.

If our adopted opacity law (Keene, Hildebrand, and Whitcomb 1982; Hildebrand 1983) is valid for the extreme density conditions found in the compact core then the column density required for an optical depth of $\tau \sim 1$ at 2.73 mm is $\sim 6 \times 10^{26}$ atoms cm^{-2} , or 1000 g cm^{-2} . This is an extraordinarily high value by the standards of molecular clouds, but it is within the range, albeit at the high end, of surface densities required for models of accretion disks around young stars (see Lin and Papaloizou 1985; Cameron 1985). The volume density of molecules is also extremely high. Even if the gas in the core had a spherical distribution, with a radius of $0''.4$, the number density would be $n_{\text{H}_2} \sim 10^{11} \text{ cm}^{-3}$. Since the material is probably flattened into a disk, the density should be significantly higher.

The size of the compact core is easy to determine from the observations. As discussed before, the upper limit from the 2.73 mm flux visibilities (Fig. 3) is 64 AU. If we assume that the 1.36 mm flux density of 0.7 Jy is due to an optically thick source, a rough lower limit to the size of the emitting region is also easily obtained. If the source temperature falls from the stellar surface as $r^{-1/2}$, more slowly than is expected for accretion disks thus giving the minimum size source, then the source radius is $\sim 0''.16$, or 25 AU. Combining this with the upper limit from observations, the radius of the compact core is therefore fairly well constrained to the range 45 ± 20 AU.

Since we have demonstrated that the compact core is a discrete, dense structure, resembling the accretion disks expected to exist around young stars, we have chosen to model it as such a thin accretion disk in order to define its characteristics in more detail. The deduced size and column density would change only slightly, however, if some other structure were assumed. This disk is embedded in the cooler envelope (of somewhat higher mass; §4.1) which serves to obscure it at short wavelengths. The structure of the source is sketched in Figure 5.

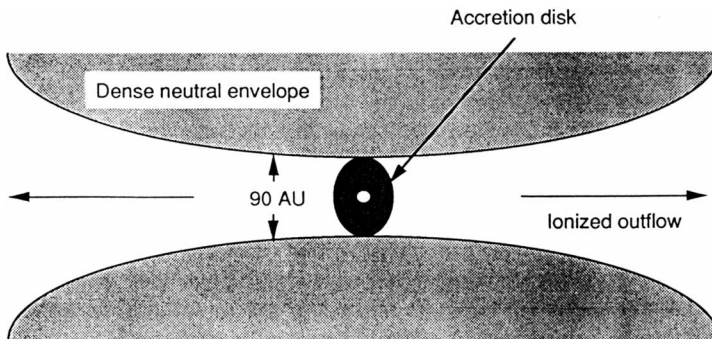


Fig. 5. Sketch of a cross-section of the neutral envelope around L1551-IRS 5, showing the embedded dense neutral disk surrounding the central star and a well-collimated ionized jet.

The theory of accretion disks around young stars is poorly understood, due to the lack

of observational constraints; many different models have been presented, with quite different physical characteristics (e.g., Cameron 1985; Safronov and Ruzmaikina 1985; Lin and Papaloizou 1985; and Hayashi, Nakazawa, and Nakagawa 1985). The temperature structure in an ideal, self-luminous, optically thick accretion disk should be a power law, with a dependence given by $T \propto r^{-3/4}$ (Lynden-Bell and Pringle 1974). Adams and Shu (1986) have shown that this distribution will be modified by radiative interaction between the star and the disk. In a deeply embedded source like L1551-IRS 5, there is a further important effect, which is due to the optically thick envelope. The ideal disk models assume that the disk radiates freely into empty space, while the presence of the envelope means that the disk is effectively inside an oven at the temperature of the inner edge of the envelope. Because radiated power is proportional to T^4 , the envelope does not have much effect on those parts of the disk which are significantly hotter than the envelope, but it sets a minimum temperature, below which the disk temperature cannot fall. We assume that the inner boundary of the envelope falls at the outer edge of the disk and, as an approximation, we assume that the envelope temperature is given by $T_{\text{env}} = T_* \times (r_*/r_{\text{env}})^{1/2}$, where T_* is the effective temperature of the star, r_* is its radius, and r_{env} is the inner radius of the envelope. Since the disk should match the stellar temperature at the surface of the star and the envelope temperature at the boundary of the envelope, we assume that the surface temperature of the disk falls as $r^{-3/4}$ out to the point where it reaches the envelope temperature and is constant thereafter. The majority of the disk area is at the temperature of the envelope. For simplicity, we ignore the details of the inner region, where grain destruction occurs, since the millimeter wave emission is insensitive to the inner boundary for temperature laws flatter than $T \propto r^{-1}$.

The calculated emission from our disk model is plotted in Figure 4, where it can be seen to reproduce the small-beam interferometric measurements quite well. The inclination of the disk was taken to be 45° (Stoche *et al.* 1988). In this model, the disk has a radius of 40 AU, a constant surface density of 840 g cm^{-2} , and a total mass of $0.6 M_\odot$. The temperature at the outer edge of the disk was 150 K. The short wavelength emission of the disk exceeds the observed values, but at these wavelengths the disk is obscured by the envelope. To demonstrate that the combination of a compact disk and a surrounding envelope can fit the observations, we have computed the continuum energy distribution of a model which consists of the disk as described above, embedded in a homogeneous spherical envelope (§4.1). The combined energy distribution is also plotted in Figure 4, where it can be seen to match the large beam measurements very well at wavelengths longer than about $40 \mu\text{m}$. The single-temperature envelope in our simple model does not reproduce the measurements at shorter wavelengths but more realistic envelope models have been discussed by Adams, Lada, and Shu (1987) and Butner *et al.* (1990).

5. Discussion

We have shown that there is a compact core to the L1551-IRS 5 cloud, centered on the radio continuum source, with a radius of $\sim 45 \text{ AU}$, an optical depth at 2.73 mm of ~ 1 , corresponding to a column density of $\sim 1000 \text{ g cm}^{-2}$, and we estimate the temperature at its outer edge to be $\sim 150 \text{ K}$. The density in this core is $n_{\text{H}_2} \gtrsim 10^{11} \text{ cm}^{-3}$, if its shape is spherical, and is higher if the structure is flattened. This source has not been seen in any other observations because of the extremely high dust opacity. We have shown that there also exists a dense envelope of material around this source with a radius $> 2000 \text{ AU}$. The two components are distinct, as can be seen in the 2.73 mm fringe visibilities.

5.1. Accretion Disks

The properties expected for circumstellar accretion disks have been discussed by many authors. Reviews of the chief competing theories are given by Cameron (1985), Safronov and Ruzmaikina

(1985), Lin and Papaloizou (1985), and Hayashi, Nakazawa, and Nakagawa (1985). Based on the properties of the planets in the solar system, it is believed that the preplanetary nebula must have had a surface density of 1000 g cm^{-2} at a radius of $\sim 1 \text{ AU}$ at the epoch of planet formation, but the total disk mass inferred depends on the radial structure. In the most parsimonious model, discussed by Hayashi, Nakazawa, and Nakagawa (1985), the surface density falls steeply with radius, and the total mass required is $0.013 M_{\odot}$. At the other extreme, the models discussed by Cameron (1985) have high surface densities which fall more slowly with radius, and correspondingly larger masses. The surface density which we estimate, $\sim 1000 \text{ g cm}^{-2}$, is comparable with the values used in the models described by Cameron (1985) and Lin and Papaloizou (1985), and the mass which we deduce within the radius of Saturn (9.5 AU) is $\sim 0.03 M_{\odot}$, in agreement with the models, but the disk radius is $45 \pm 20 \text{ AU}$, and the total mass is therefore much larger than that of a minimum mass solar nebula.

Thus, the compact core centered on L1551–IRS 5 has properties very close to those expected for accretion disks around young stars, and we therefore believe that the most plausible hypothesis is that it is such a disk. Definite confirmation of this hypothesis will require further observations to map the structure of the source and to detect the velocity signature of Keplerian rotation to demonstrate that the material is in orbit around IRS 5.

5.2. Envelope Structure

It is obvious from optical, near-infrared, molecular line, and radio observations that the envelope surrounding IRS 5 does not have the spherical symmetry we have assumed for simplicity in our modeling. IRS 5 lies at the center of a large molecular outflow (Snell, Loren, and Plambeck 1980) and at the center of an ionized jet, visible at radio (Bieging and Cohen 1985) and optical (Mundt and Fried 1983; Campbell *et al.* 1988) wavelengths. Near-infrared observations reveal a conical structure that has been interpreted to be reflection from the inner edge of a thick disk (Strom *et al.* 1985; Hodapp *et al.* 1988). This infrared structure is larger than the disk revealed by our interferometer observations but could easily be the inner edge of the dense neutral envelope. The implied lack of spherical symmetry of the envelope does not affect our analysis of the compact core, nor does it change our estimate of the envelope mass. Our 1.25 mm CSO observations do not reveal any departure from spherical symmetry of the envelope on the $\sim 20''$ scale nor do the high-resolution 50 and $100 \mu\text{m}$ observations of Butner *et al.* (1990).

6. Conclusions

We have made high-resolution observations of the millimeter-wave continuum emission from L1551–IRS 5. At a wavelength of 2.73 mm we have detected a compact core with a radius of $\leq 0''.4$ ($\leq 64 \text{ AU}$) which accounts for about half of the total continuum flux density at this wavelength. The most likely explanation for this source is that it is an accretion disk surrounding the central star.

From a single-dish map at a wavelength of 1.25 mm, we demonstrate that the compact core is surrounded by an envelope with a radius $\geq 12''$. We estimate that the mass of the envelope is $2 - 3 M_{\odot}$.

The spectrum of the continuum emission from the compact core is very flat and is consistent with optically thick thermal emission for wavelengths shorter than 2.73 mm. If our adopted opacity law is valid for the compact core and if the 2.73 mm optical depth is ~ 1 , then the column density in the compact core is $N_{\text{H}} \approx 6 \times 10^{26} \text{ atoms cm}^{-2}$, or $\sim 1000 \text{ g cm}^{-2}$. This is much larger than any column densities previously measured in neutral material, but it is comparable with column densities predicted in models of accretion/preplanetary disks around young stars. The radius of

the compact core closely matches the expected size of an accretion disk around the young star and the size of our own solar system.

With the aid of a simple disk model we have shown that the radius of the compact core is 45 ± 20 AU, and that the total mass is $\sim 0.6 M_{\odot}$. This mass is larger than expected in most models of presolar systems, largely because the surface density is somewhat high, but in the course of the evolution of such a system, much of the material may yet be accreted on to the star or blown off in the wind.

The OVRO millimeter interferometer is supported by NSF grant AST 87-14405 to Caltech; the CSO is supported by NSF grant AST 88-15132 to Caltech.

References

- Adams, F. C., Lada, C. J., and Shu, F. H. 1987, *Ap. J.*, **312**, 788.
- Adams, F. C., and Shu, F. H. 1986, *Ap. J.*, **308**, 836.
- Bieging, J. H., and Cohen, M. 1985, *Ap. J. (Letters)*, **289**, L5.
- Bieging, J. H., Cohen, M., and Schwartz, P. R. 1984, *Ap. J.*, **282**, 699.
- Butner, H. M., Evans, N. J., II, Lester, D. F., Levreault, R. M., and Strom, S. E. 1990, *Ap. J.* in press.
- Cameron, A. G. W. 1985, in *Protostars and Planets II*, ed. D. C. Black and M. S. Matthews (Tucson: University of Arizona Press), p. 1073.
- Campbell, B., Persson, S. E., Strom, S. E., and Grasdalen, G. L. 1988, *A. J.*, **95**, 1173.
- Draine, B. T., and Lee, H. M. 1984, *Ap. J.*, **285**, 89.
- Hayashi, C., Nakazawa, K., and Nakagawa, Y. 1985 in *Protostars and Planets II*, ed. D. C. Black and M. S. Matthews (Tucson: University of Arizona Press), p. 1100.
- Hildebrand, R. H. 1983, *Quart. J. R. A. S.*, **24**, 267.
- Hodapp, K.-W., Capps, R. W., Strom, S. E., Salas, L., and Grasdalen, G. L. 1988, *Ap. J.*, **335**, 814.
- Keene, J., Hildebrand, R. H., and Whitcomb, S. E. 1982, *Ap. J. (Letters)*, **252**, L11.
- Lin, D. N. C., and Papaloizou, J. 1985, in *Protostars and Planets II*, ed. D. C. Black and M. S. Matthews (Tucson: University of Arizona Press), p. 981.
- Lynden-Bell, D., and Pringle, J. E. 1974, *M. N. R. A. S.*, **168**, 603.
- Mundt, R., and Fried, J. W. 1983, *Ap. J. (Letters)*, **274**, L83.
- Mundt, R., Stocke, J., Strom, S. E., Strom, K. M., and Anderson, E. R. 1985, *Ap. J.*, **297**, L41.
- Rodríguez, L. F., Cantó, J., Torrelles, J. M., and Ho, P. T. P. 1986, *Ap. J. (Letters)*, **301**, L25.
- Safronov, V. S., and Ruzmaikina, T. V. 1985, in *Protostars and Planets II*, ed. D. C. Black and M. S. Matthews (Tucson: University of Arizona Press), p. 959.
- Sargent, A. I., and Beckwith, S. 1987, *Ap. J.*, **323**, 284.
- Smith, B. A., and Terrile, R. J. 1985, *Science*, **226**, 1421.
- Snell, R. L. 1981, *Ap. J. Suppl.*, **45**, 121.
- Snell, R. L., Loren, R. B., and Plambeck, R. L. 1980, *Ap. J. (Letters)*, **239**, L17.
- Stocke, J., Hartigan, P. M., Strom, S. E., Strom, K. M., Anderson, E. R., Hartmann, L. W., and Kenyon, S. J. 1988, *Ap. J. Suppl.*, **68**, 229.
- Strom, S. E., Strom, K. M., Grasdalen, G. L., Capps, R. W., and Thompson, D. 1985, *A. J.*, **90**, 2575.

Terebey, S., Shu, F. H., and Cassen, P. 1984, *Ap. J.*, **286**, 529.

Walker, C. K., Adams, F. C., and Lada, C. J. 1990, *Ap. J.*, **349**, 515.

Woody, D. P., Scott, S. L., Scoville, N. Z., Mundy, L. G., Sargent, A. I., Padin, S.,
Tinney, C. G., and Wilson, C. D. 1989, *Ap. J. (Letters)*, **337**, L41.